Journal of Applied Polymer Science

Rheological Behaviors of Fumed Silica/Low Molecular Weight Hydroxyl Silicone Oil

Guo-Dong Zhang,[1,2] Ji-Rong Wu,[2] Long-Cheng Tang,[2] Jia-Yun Li,[2] Guo-Qiao Lai,[1,2] Ming-Qiang Zhong[1]

[1]College of Chemical Engineering and Materials, Zhejiang University of Technology, Hangzhou 310014, China

[2]Key Laboratory of Organosilicon Chemistry and Material Technology of Ministry of Education, Hangzhou Normal University, Hangzhou 310012, China

Correspondence to: G.-Q. Lai (E-mail: zgd830@sina.com) and M.-Q. Zhong (E-mail: zhongmq@zjut.edu.cn)

ABSRACT: The structure and viscoelastic properties of fumed silica gels in low molecular weight hydroxyl silicone oil were investigated by means of steady and dynamic rheology. It is found that the fumed silica/hydroxyl silicone oil suspension exhibits shear-thickening under steady shear and "strain-thickening" under oscillatory shear condition. Effects of hydroxy groups on the rheological behavior of silicone oil suspension with highly dispersed hydrophilic amorphous silica were investigated by infrared, ^{1}H-NMR, and rheological test. The results show that the hydroxy groups on this system play an important role on the formation of shear thickening behavior of the suspension solution. At the same particle diameter and mass fraction, the amount of hydroxy groups on this system has a strong effect on increasing the viscosity of the suspension, which is likely due to multiassociation hydrogen bonding between liquid molecules and silanol groups on fumed silica surfaces (Si—OH). © 2014 Wiley Periodicals, Inc. J. Appl. Polym. Sci. **2014**, *131*, 40722.

KEYWORDS: blends; composites; property relations; structure

Received 26 November 2013; accepted 11 March 2014
DOI: 10.1002/app.40722

INTRODUCTION

In general, polymers can be endowed with a great quantity of advantages after incorporation of inorganic filler particles into them, such as increased strength and electrical conductivity over the pure polymer systems.[1] When the particle size reaches the nanoscale (less than 100 nm), the nanofiller/polymer material is commonly referred to as a polymer nanocomposite.[2] During the past decade, the polymer nanocomposites have attracted considerable attentions in both the academic interests and industrial fields such as paints, foods, cosmetics, sealants, and automobile tire tread compound,[1,3] shear thickening fluids (STFs) in particular.[4–10] STFs usually made of highly concentrated colloidal suspensions of rigid particles, are characterized by an increase in effective viscosity when the shear rate increases past a certain critical value. Initial interest in shear thickening arose from its association with damage to processing equipment and dramatic changes in suspension microstructures, resulting in the destruction of equipments like pumps or stirrers.[5,9]

STFs are concentrated colloidal suspensions and composed of nonaggregating inorganic particles suspended in fluids, showing a significant increase in viscosity beyond a critical shear rate. As reported in the studies of Hoffman[11,12] and others,[8,13,14] it is well established that two microstructural models are usually used to explain shear-thickening phenomenon, i.e. the order-disorder transition (ODT) theory and the cluster-formation theory. In addition, the increased viscosity of STFs is characteristics of both reversible and "field activated," which depends on the applied shearing rate.[15] It is well established that this increased viscosity is the consequence of the formation of jamming clusters bound together by hydrodynamic lubrication forces, often denoted by the term of hydroclusters.[3,15] The rheological behaviors of STFs is influenced by a variety of parameters,[16] including the particle size distribution, particle shape, volume fraction, particle–particle interactions, and the viscosity of the suspending phase.[9]

Recently, an increasing number of applications take advantage of the shear thickening behavior to improve the related performance.[4,5] A representative example is that the incorporation of STFs to Kevlar fabrics improved their ballistic protection capabilities[1,4] and the stab resistance,[5–8] which has been exploited for the design of damping, control devices, etc.

In this work, the STFs composed of nanosize silica particles suspended in low molecular weight hydroxyl silicone oil (LMWHSO) were prepared. Their steady and oscillatory shear behaviors were preformed by using a rheometer. The microstructure and rheological characteristic of the fumed silica/LMWHSO

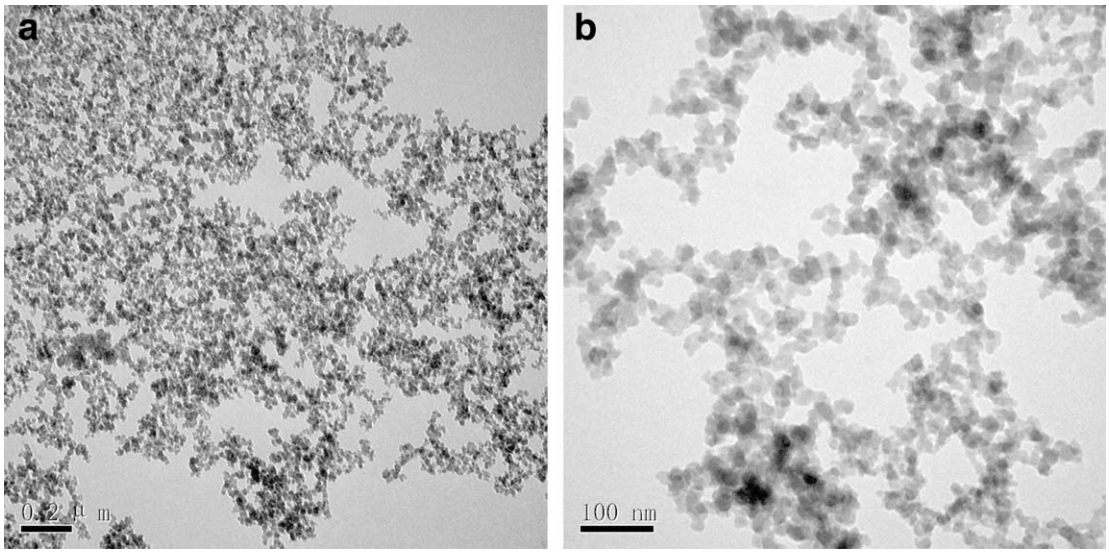

Figure 1. TEM images of the fumed silica aggregates observed at different magnifications, displaying chain-like structure in LMWHSO.

have been studied at different particle loadings and silazane modification conditions. This work focused on elucidating the colloidal interactions that dictates the microstructures in the silica/LMWHSO system.

EXPERIMENTAL

Materials

Silica nanoparticles with 150 m^2/g nm of specific surface area (BET) were supplied by Guangzhou GBS High-Tech & Industry Corporation, China. The nanoparticles are colloidal and hydrophilic particles due to the abundance of silanol groups on their surfaces. Fumed silica i.e., pyrogenic silica is produced in a flame which consists of microscopic droplets of amorphous silica fused into branched, chainlike, three-dimensional secondary particles which then agglomerate into tertiary particles.[17] Variation of the processing parameters (flame temperature, residence time) allows the synthesis of silica with the BET ranging from 50 to 400 m^2/g. The nature of the surface of the fumed silica aggregates, to a large extent, determines the gelling behavior of the dispersions. The untreated fumed silica particles were also used in this study. Prior to use in dispersions, the fumed silica particles were dried for 12 h in a vacuum oven at 120°C.[18] The hydroxyl-terminated polydimethylsiloxane (PDMS) having a viscosity of 25cs at 25°C, was a commercially available product from GE Toshiba Silicones, Japan. 1,1,1,3,3,3-Hexamethyldisilazane (HMDS) were supplied by Hangzhou Dayangchem, China.

Preparation of the Silica/LMWHSO Suspension

The fumed silica nanoparticles were added into LMWHSO at a different amount of fumed silica by using a planetary mixer (Foshan Golden Milky Machinery China) with a rotor speed of 50 rpm at room temperature. The mixing was conducted as following: (1) LMWHSO was first added into the planetary mixer and softened for 10 min without addition of filler; (2) then the fumed silica was added and mixed for 60 min; (3) after that, the mixture was mixed for ~90 min in Planetary Ball Mill PM 400 to ensure a good dispersion of nanofillers.[19–21] After degassing, the suspension samples were put in a plastic cylinder (200 mL) for storage and measurements. Different loadings of fumed silica nanoparticles (10–45 phr) in LMWHSO was prepared under the same conditions and was named following the particle content loading of silica.

Silazane Treatment

The processing conditions of silazane modification samples were made as following: about 10 wt % HMDS was added into the untreated samples, and then was kept at 110°C and 2 h for the reaction; finally, the silazane-modified samples were obtained after taking off the low weight molecular compound for 2 h in vacuum.

Characterization

Untreated and silazane-modified samples were analyzed with a Nicolet 5700 Fourier-transform infrared spectroscopy (FTIR). ^{1}H-NMR spectra were measured using a Bruker AV400 MHz spectrometer operating at 400.13 MHz. The particle sizes and distributions of the prepared silica/LMWHSO suspension were directly measured using a dynamic light scattering (DLS, BI-200SM Brook, USA). Each sample was analyzed three times and average experimental results were reported. The microstructure and morphology of the prepared particles were examined by a transmission electron microscopy (TEM, HITACHI H-7650) operated at 80 kV. The samples were diluted with ethanol by low speed mixing before testing and then collected on carbon-coated 200-mesh copper grids for TEM observation. Considering the fact that the dilution process is similar as the shear process, the dispersion level observed by the TEM observation can reflect the silica dispersion in LMWHSO.

Dynamic rheological tests were carried out using a stress controlled rotational rheometer (AR2000, TA Instruments) with parallel plates (25 mm in diameter). The rheometer is equipped with a Peltier control system that provides accurate control of temperature (±0.1°C). In the process of sample loading and dynamic rheological tests, care and some measures are required to minimize any possible damage of the network and to keep it

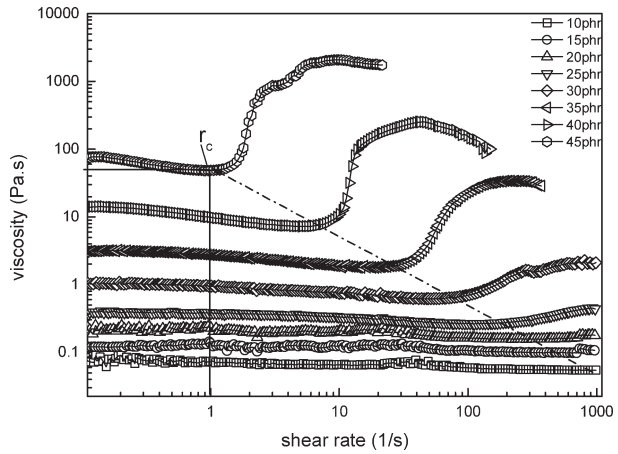

Figure 2. Viscosity as a function of shear rate for fumed silica/LMWHSO at various particle loadings.

intact. For the sample loading, two measures were adopted to reduce the destruction of the gels. First, the sample was poured into the plates from the fixed volume scoop, (a sample volume of 0.5 mL was chosen in this work); Second, the speed and the force of the compression process to produce an appropriate gap (1.00 mm) for the dynamic rheological experiments were strictly controlled by the rheometer. Moreover, before each dynamic test, a steady preshear was applied at a shear rate of 0.1 s^{-1} for 30 s followed by a 180 s resting period. This procedure is necessary to erase any previous shear histories on the sample and to ensure that the sample establishes its equilibrium structure.[18] With these measures, the experimental data were found to be reproducible with a relative error of <8%.

RESULTS AND DISCUSSION

Structural Characterization

Figure 1 contains the representative TEM images of the silica/LMWHSO suspension. As shown in Figure 1(a), the fumed silica nanoparticles display the chain-like structure, which is formed by these quasi-spherical primary silica particles. Although the relatively highly dispersed silica nanoparticles seem to be obtained after the use of the high shear mechanical mixing, some small agglomerations of the silica still presents in the LMWHSO [Figure 1(b)], which is hardly disrupted into primary particles.

Rheological Behavior

Steady-State Rheological Behavior. Figure 2 shows the steady-state rheological behavior of fumed silica nanoparticle suspensions of various filler loadings. In all cases, shear thinning at low shear rates is followed by shear thickening at higher shear rates. The strength of the shear thickening response increases as particle loading increases, with discontinuous shear thickening at the highest particle loadings. The critical shear rate (r_c) at which initiates the shear thickening behavior shows significant decrease with increasing particle loading. (The r_c indicates the critical shear rate above which the suspensions show a significant increase in the viscosity.) For these suspensions with relatively high filler content of silica nanoparticles, the maximum viscosity above the r_c increases by an order of magnitude over that below the r_c value.

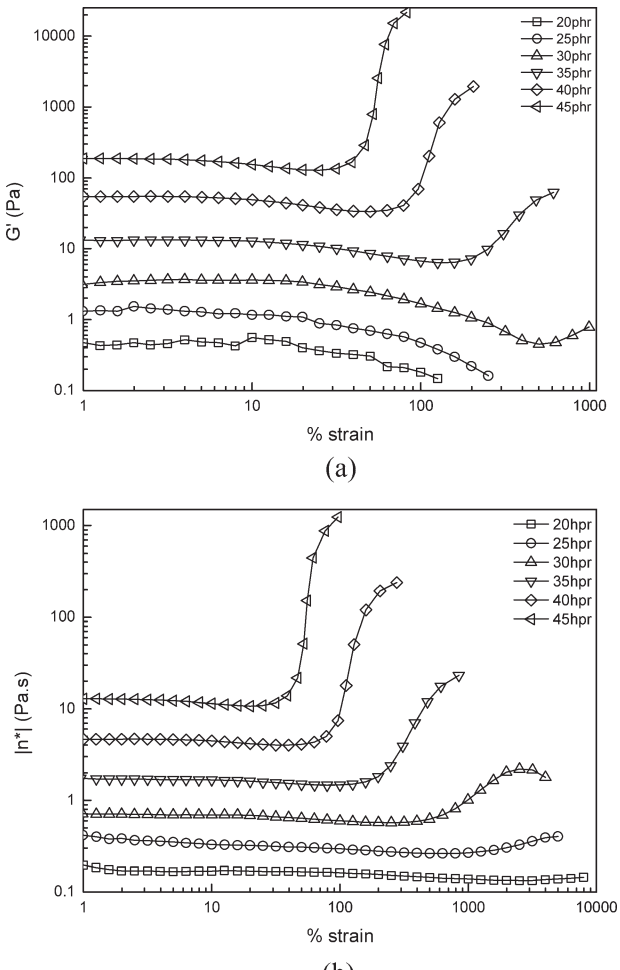

Figure 3. (a) Storage modulus (G') and (b) complex viscosity (η^*) of the LMWHSO suspensions containing different weight fractions of fumed silica. (The strain sweeps were conducted at 20 rad/s and 25°C.)

Strain-Thickening Behavior Under Dynamic Shear. The viscoelastic behavior of different weight fractions of fumed silica suspension in LMWHSO is illustrated in Figure 3(a) in terms of a strain sweep. The experiment was performed from low to high amplitude strains at a constant frequency of 20 rad/s. Strain sweeps were conducted at several particle volume fractions and are plotted in Figure 3. The linear viscoelastic response of such dispersions typically shows sol-like behavior: the elastic moduli (G') [Figure 3(a)] depend strongly on strain. This can also be observed in the complex viscosity η^*, which is simply the complex modulus G^* divided by the frequency of the deformation.

An increase in $|\eta^*|$ corresponds to a larger torque response exerted by the sample, and the phenomenon was explained to be flow-blocking reported in the previous work.[13] The results in Figure 3 indicate that the transition of the strain-thickening (flow-blocking) behavior occurs at smaller strains as the particle loading increases. As shown in Figure 3(b), the LMWHSO-based suspension exhibits strain-thickening at high strain amplitudes, with both the G' and the η^* showing an abrupt jump to higher levels at a particular strain.

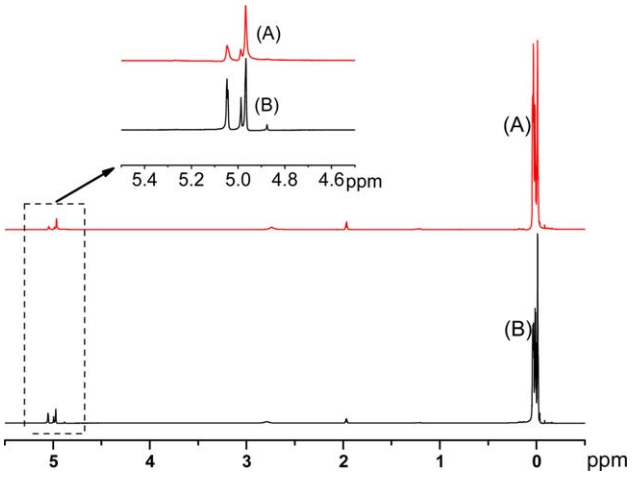

Figure 4. [1]H-NMR spectra of untreated sample and silazane-modified sample. (a) Silazane-modified sample, (b) untreated sample. [Color figure can be viewed in the online issue, which is available at wileyonlinelibrary.com.]

Clustering Mechanism for Shear-Thickening. The preceding correlation between shear-thickening (steady) and strain-thickening (dynamic) shows that the two phenomena are closely related in terms of their underlying mechanism. Two main theories i.e., the ODT and clustering formation have been used to explain the shear-thickening phenomenon. Notably, the mechanism of ODT indicates that the incipience of shear-thickening at a critical shear rate (r_c) corresponds to a transition from an easy flowing state where the particles are ordered into layers to a disordered state where this ordering is absent. Previous work reported that the clustering mechanism should be a more accurate and generalized model in comparison with the ODT mechanism, although the later could be a concomitant effect in many cases.[15,22]

The formation of ordered particle layers is easy to visualize if the suspended particles conform to regular shapes, such as spheres or rods. In most of the classical studies on shear-thickening,[1,4–6] the particles in suspension were monodisperse spheres, stabilized either electrostatically or sterically. Thus, it is highly probable that the suspensions in these studies can show ordering at low shear rates. However, in our case, the primary flow units in the suspension are aggregates and not individual particles of silica. The silica aggregates are irregular, anisotropic structures (Figure 1), which can be modeled as fractals. The aggregates may range in size from 50 nm to 0.5 μm and cannot be disrupted by shear into the primary particles. It seems unlikely that these irregular, polydisperse structures can be arranged into ordered layers at low shear rates.

Effect of OH Density

In the [1]HNMR spectra (Figure 4), the band in the spectra of untreated samples at around 5 is assigned to the presence of hydroxyl radical. Untreated samples contain a great deal of hydroxyl radical. In the [1]HNMR spectra, the amount of hydrogen bonds for silazane-modified samples obviously decreased. It has been shown that the silazane-modified samples contains fewer hydrogen bonds than the untreated samples.

FTIR spectroscopy is a powerful characterization technique for examining the chemical structure of polymer nanocomposite.[23]

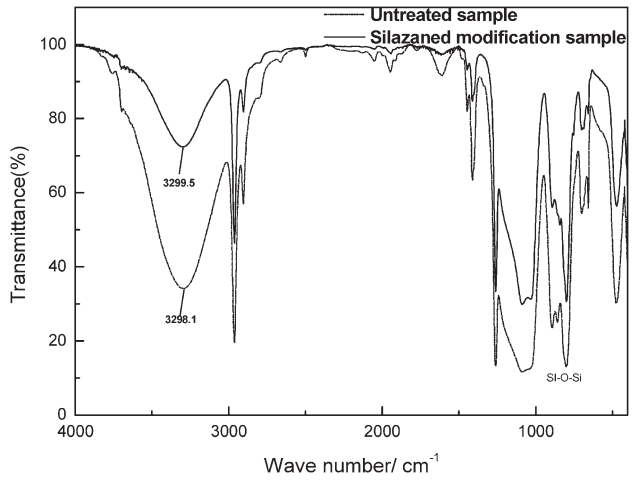

Figure 5. FTIR spectra of untreated and silazane-modified samples.

Figure 5 shows the FTIR spectra of untreated and silazane-modified samples. The band presents in the diffuse reflection infrared Fourier-transform spectra of untreated samples at 3298.1 cm^{-1}, is assigned to the hydroxyl radical. The spectrum also shows the band for silazane-modified samples present at 3299.5 cm^{-1}, and the form of peak becomes narrow and acute. As shown in Figure 5, the untreated samples contain a great deal of hydrogen bonds. In contrast, the OH peak appears significantly smaller in the silazane-modified samples. In fact, the peak ratio of this OH band to other fixed band (such as the Si—O—Si band) also exhibits a decrease after the silazane modification (see Figure 5). This further demonstrates that the number of hydroxyls has decreased after the silazane modification process. That is to say, the silazane-modified samples contains fewer hydrogen bond than untreated samples.[24]

Comparison of Shear Thickening Ability

Fumed silica suspension in LMWHSO exhibits shear thickening at higher shear rates. Figure 6 shows the strength of the shear thickening response increases as OH density of the system increases. The critical shear rate (r_c) at which initiates the shear

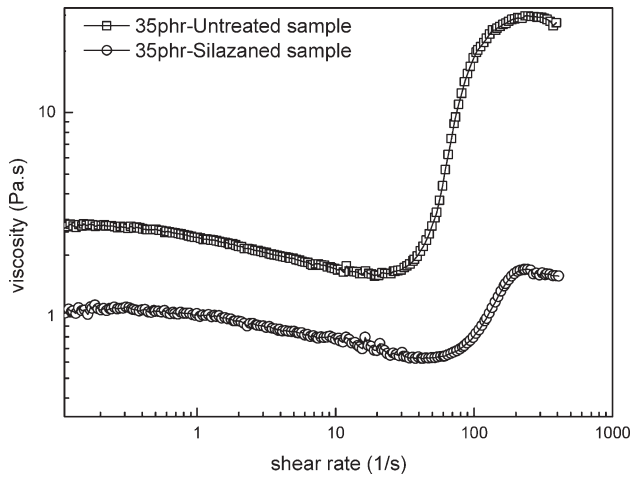

Figure 6. Viscosity as a function of shear rate for fumed silica/LMWHSO with untreated and silazane-modified procedures.

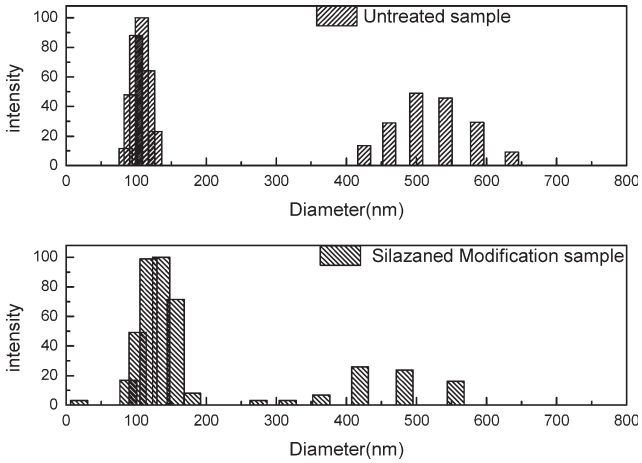

Figure 7. Size distribution for untreated and silazane-modified samples using APD detector in 90 Plus.

thickening behavior shows significant decrease with increasing OH density of the system. At the same particle diameter and mass fraction, the decreased amount of hydroxy groups in the STFs impaired the shear thickening effect.

Comparison of Particle Sizing

The measurement of particle size using dynamic light scattering, also known as photon correlation spectroscopy, is well known. Scattered laser is auto correlated, fit either with cumulants to determine moments of the distribution, or with more sophisticated algorithms to determine the shape of the distribution. With appropriate laser power and scattering angles, sizes from 1 nm to a couple of microns have been determined.[25]

Comparison with patterns of untreated sample's particle size (Figure 7) shows that agglomeration of silazane-modified samples is slightly weaker. It is possible that the silazane-modified samples contains fewer hydrogen bonds than untreated samples, but patterns of particle size distribution undergo little overall change.

CONCLUSIONS

In this work, the structure and viscoelastic properties of fumed silica gels in LMWHSO were investigated and the relative mechanisms were discussed. Fumed silica suspensions in LMWHSO exhibited shear-thickening under steady flow, and strain-thickening under oscillatory shear. The combined shear- and strain-thickening behaviors were also investigated to understand the relative clustering mechanism, which would attribute to the thickening phenomena after the presence of temporary, flow-induced clusters. Under the steady shear or oscillatory shear at high amplitudes the connection of aggregates into clusters readily could occur. Effects of hydroxy groups on the rheological behavior of high content dispersion suspension solution of hydrophilic amorphous silica dispersed in LMWHSO were investigated by infrared, ^{1}H-NMR. The results showed that the hydroxy groups on the STFs play an important role on the formation of shear thickening behavior of suspension solution. At the same particle diameter and mass fraction, the decreased amount of hydroxy groups in the STFs impaired the shear thickening effect.

ACKNOWLEDGMENTS

The authors thank the Natural Science Foundation of China (21303036, 21203049) and the Foundation of Zhejiang Educational Committee (Y201327588) for financial support.

REFERENCES

1. Xu, X. M.; Tao, X. L.; Gao, C. H.; Zheng Q. *J. Appl. Polym. Sci.* **2008**, *107*, 1570.
2. Anderson, B. J.; Zukoski, C. F. *Macromolecules* **2008**, *41*, 9326.
3. Galindo-Rosales, F. J.; Moldenaers, P.; Vermant, J. *Macromol. Mater. Eng.* **2011**, *296*, 331.
4. Fischer, C.; Bennani, A.; Michaud, V.; Jacquelin, E.; Manson, J. E. *Smart Mater. Struct.* **2010**, *19*, 1.
5. Galindo-Rosales, F. J.; Rubio-Hernández, F. J.; Sevilla, A. J. *Non-Newton. Fluid.* **2011**, *166*, 321.
6. Xu, Y. L.; Gong, X. L.; Peng, C.; Sun, Y. Q.; Jiang, W. Q.; Zhang, Z. *Chinese J. Chem. Phys.* **2010**, *23*, 342.
7. Galindo-Rosales, F. J.; Rubio-Hernández, F. J.; Velázquez-Navarro, J. F. *Rheol. Acta* **2009**, *48*, 699.
8. Lee, Y. S.; Wetzel, E. D.; Wagner, N. J. *J. Mater. Sci.* **2003**, *38*, 2825.
9. Chang, L.; Friedrich, K.; Schlarb, A. K.; Tanner, R.; Ye, L. *J. Mater. Sci.* **2011**, *46*, 339.
10. Munoz, M. E.; Santamaria, A.; Guzman, J.; Riande, E. *J. Rheol.* **2003**, *47*, 1041.
11. Hoffman, R. L. *J. Rheol.* **1972**, *16*, 155.
12. Hoffman, R. L. *J. Colloid. Interf. Sci.* **1974**, *46*, 491.
13. Boersma, W. H.; Laven, J.; Stein, H. N. *J. Colloid. Interf. Sci.* **1992**, *149*, 10.
14. Catherall, A. A.; Melrose, J. R.; Ball, R. C. *J. Rheol.* **2000**, *44*, 1.
15. Zhang, X. Z.; Li, W. H.; Gong, X. L. *Smart Mater. Struct.* **2008**, *17*, 27.
16. Raghavan, S. R.; Walls, H. J.; Khan, S. A. *Langmuir* **2000**, *16*, 7920.
17. Nordstrom, J.; Matic, A.; Sun, J.; Forsyth, M.; MacFarlane, D. R. *Soft Matter* **2010**, *6*, 2293.
18. Wu, X. J.; Wang, Y.; Wang, M.; Yang, W.; Xie B. H.; Yang, M. B. *Colloid. Polym. Sci.* **2012**, *290*, 151.
19. Tang, L. C.; Wan, Y. J.; Peng, K.; Pei, Y. B.; Wu, L. B.; Chen, L. M. *Compos. Part A* **2013**, *45*, 95.
20. Wan, Y. J.; Tang, L. C.; Yan, D.; Zhao, L.; Li, Y. B.; Wu, L. B. *Compos. Sci. Technol.* **2013**, *82*, 60.
21. Tang, L. C.; Wan, Y. J.; Yan, D.; Pei, Y. B.; Zhao, L.; Li, Y. B. *Carbon* **2013**, *60*, 16.
22. Xu. S. P.; Zhang, Y. F. *Bull. Chin. Ceram. Soc.* **2011**, *30*, 966.
23. Sumi, D.; Dhanabalan, A.; Thimmappa, B. H. S.; Krishnamurthy, S. *J. Appl. Polym. Sci.* **2012**, *125*, E515.
24. Ramos, M. A.; Gil, M. H.; Schacht, E.; Matthys, G.; Mondelaers, W.; Figueiredo, M. M. *Powder Technol.* **1998**, *99*, 79.
25. Finsy, R. *Adv. Colloid. Interface* **1994**, *52*, 79.